

---

# Hybrid Adversarial Inverse Reinforcement Learning

---

Mingqi Yuan<sup>1,2</sup>    Man-on Pun<sup>1,2,3</sup>    Yi Chen<sup>1,2</sup>

<sup>1</sup>The Chinese University of Hong Kong, Shenzhen

<sup>2</sup>Shenzhen Research Institute of Big Data

<sup>3</sup>Shenzhen Key Laboratory of IoT Intelligent System and Wireless Network Technology

[mingqiyuan@link.cuhk.edu.cn](mailto:mingqiyuan@link.cuhk.edu.cn)

[{simonpun,yichen}@cuhk.edu.cn](mailto:{simonpun,yichen}@cuhk.edu.cn)

## Abstract

Extrapolating beyond-demonstrator (BD) through the inverse reinforcement learning (IRL) algorithm aims to learn from and outperform the demonstrator. In sharp contrast to the conventional reinforcement learning (RL) algorithms, BD-IRL can overcome the dilemma incurred in the reward function design and solvability of the RL, which opens new avenues to building superior expert systems. Most existing BD-IRL algorithms are performed in two stages by first inferring a reward function before learning a policy via RL. However, such two-stage BD-IRL algorithms suffer from high computational complexity, low robustness and large performance variations. In particular, a poor reward function founded in the first stage will inevitably incur severe performance loss in the second stage. In this work, we propose a hybrid adversarial inverse reinforcement learning (HAIRL) algorithm that is one-stage, model-free, generative-adversarial (GA) fashion and curiosity-driven. Thanks to the one-stage design, the HAIRL can integrate reward function learning and policy optimization into one procedure, which leads to many advantages such as low computational complexity, high robustness, and strong adaptability. More specifically, HAIRL simultaneously imitates the demonstrator and explores BD performance by utilizing hybrid rewards. In particular, the Wasserstein distance (WD) is introduced in HAIRL to stabilize the imitation procedure while a novel end-to-end curiosity module (ECM) is developed to improve exploration. Finally, extensive simulation results confirm that HAIRL can achieve higher performance as compared to other similar BD-IRL algorithms. Our code is available at our website<sup>1</sup>.

## 1 Introduction

Reinforcement learning (RL) is widely applied in building expert systems (e.g., AlphaZero and AlphaStar) due to its powerful learning and exploration ability [1, 2]. However, the RL is also increasingly showing its critical flaw in practice. On the one hand, the reward signal is always sparse or missing in many real-world scenarios, and it is impossible to construct a shaped reward function [3]. Even if an artificial reward function is obtained, it can not be mathematically proven correct and efficient. On the other hand, it is also challenging to guarantee the solvability of the RL, because high-dimensional observation space induces massive searching space. As a result, it leads to high computational complexity when realizing the convergence of the RL model.

To cope with the problem of reward function, the inverse reinforcement learning (IRL) is developed to infer a reward function by learning from some demonstrations [4]. For instance, a sophisticated

---

<sup>1</sup><https://github.com/yuanmingqi/HAIRL>

driver is thought to have some secrets that lead him to drive well. The IRL formulates such secrets as an explicit reward function so that the driver can get feedback and adjust his driving policy. Based on the inferred reward function, the policy of the expert can be recovered via RL [5]. However, the learned policy is consistently found to be sub-optimal and intractable to outperform the expert [6]. This is because the IRL only aims to find the reward function that makes the demonstrations appear optimal, which does not make any efforts to improve the policy [7]. But if we can build stronger reward function through IRL, it is feasible to imitate and outperform the demonstrator.

Learning from the demonstrator and outperform the demonstrator via IRL is entitled as beyond-demonstrator (BD) IRL. [6] first proposed the concept of extrapolating BD performance via IRL and designed a trajectory-ranked reward extrapolation (TREX) framework. The TREX first collects a series of ranked trajectories and then trains a parameterized reward function to make the rank relation accurate. Finally, the reward function is taken to train the agent via RL. By fully exploring the reward space, the TREX provides a high-quality reward function to learn BD policies. In [8], the TREX is further expanded to the multi-agent task, and an MA-TREX is proposed. It is challenging to get well-ranked trajectories for TREX, thus [9] proposed a disturbance-based reward extrapolation (DREX) framework, which can automatically generate the ranked demonstrations by injecting noise through the policy learning. Both the TREX and DREX suffer from the requirement of enough demonstrations. To address the problem, [7] proposed a generative intrinsic reward-driven imitation learning (GIRIL) framework, which took one-life demonstration to learn a family of reward functions using variational autoencoder (VAE) [10]. [7] first introduced the curiosity module (CM) to the BD-IRL to explore BD performance. The simulation results show that the GIRIL can learn a BD policy at the cost of fewer demonstrations. All the discussed algorithms above are two-stage, which first learn a specialized reward function then explore the BD policy via RL. However, these algorithms suffer from high computation complexity and produce more variance because of the two separate procedures. In particular, a poor reward function founded in the first stage would inevitably incur severe performance loss in the second stage.

Inspired by the discussions above, we consider building a one-stage BD-IRL algorithm, learning the reward function and optimizing the policy simultaneously. To our best knowledge, there is no existing one-stage BD-IRL framework yet. In contrast to the two-stage algorithms, the reward function is updated dynamically to adapt to the varying learning process, which has higher generalization and robustness. In particular, the one-stage architecture will significantly promote the efficiency, the reward function and policy are simultaneously obtained once the training is completed. In this paper, we propose the hybrid adversarial inverse reinforcement learning (HAIRL), which is a model-free, one-stage, GA fashion and curiosity-driven IRL algorithm. The HAIRL uses two independent modules for behavior imitation and policy exploration: extrinsic reward block (ERB) and intrinsic reward block (IRB). The two modules generate a hybrid reward signal to update the policy, realizing imitation and exploration simultaneously. The simulation results show that the HAIRL outperforms the similar state-of-the-art (SOTA) algorithms.

## 2 Related Work

**Inverse reinforcement learning.** The dilemma of reward function design promotes the development of the IRL. The IRL aims to find a reward function that explains the demonstrations which are thought to be drawn from an optimal demonstrator [4]. Taking the inferred reward function, an optimal policy can be recovered via RL [5]. Many IRL algorithms have been developed both for single-agent and multi-agent tasks based on deep learning, information theory and probability theory, etc [11, 12, 13, 14, 15, 16, 17, 18]. For instance, the maximum entropy (ME)-IRL seeks to find a reward function that makes the demonstrations satisfy the principle of ME [11]. More specifically, the ME-IRL assumes the probability of choosing a trajectory is proportional to the sum rewards in this trajectory. Finally, the MR-IRL learns the reward function via maximum likelihood estimation (MLE). However, these methods only seek a reward function that justifies the demonstrations, which is intractable to outperform the demonstrator.

Based on the ME assumption, [19] proves the connection and equivalence between IRL and GA network (GAN) [20]. [21] subsequently proposed the adversarial IRL (AIRL) that solves the IRL problem using GA fashion. In AIRL, the agent serves as the generator for producing trajectories, and the discriminator evaluates whether the trajectories are from the expert. Then the discriminator score is used as the reward to train the agent to imitate the expert. In particular, AIRL obtain the

reward function and recovered policy simultaneously, which has low computation complexity and high robustness. In our work, we inherit the insight of AIRL and redesign the reward module to build the one-stage BD-IRL algorithm.

**Curiosity-driven reinforcement learning.** Our work is also related to the research on the curiosity-driven learning. There are two kinds of reward signal in RL, namely the extrinsic reward signal (ERS) and intrinsic reward signal (IRS) [22]. The ERS is usually given by the environment explicitly, such as the time cost in the Mountain-Car game. On the opposite, the IRS represents the intrinsic learning motivation/curiosity of the agent, which is an implicit and fuzzy concept. Much prior work has been done to formally formulate the IRS, and it can be broadly sorted into two classes. One is to encourage the agent to explore novel state as much as possible [23, 24]. The other one drives the agent to reduce the uncertainty in predicting the consequent actions [25, 26, 27, 28]. [29] first build a practical and general module entitled intrinsic curiosity module (ICM), which provides IRS using an attendant model. Given a transition, this model predicts a next-state based on the current state-action pair. Finally, the prediction error is taken to be the IRS, and it will be added with the ERS to form a mixed reward. To some extent, the utilization of the IRS solves the problem of sparse reward signal. In particular, [30] proves that the agent can learn considerable policy only using IRS in extensive experiments. In this work, we introduce the CM in our framework, motivating the agent to make more explorations and realize BD performance. Moreover, we propose a novel ECM which has simple architecture but higher performance.

### 3 Preliminaries

We study the BD-IRL problem considering the Markov decision process (MDP) defined by a tuple  $\mathcal{M} = \langle \mathcal{S}, \mathcal{A}, \mathcal{T}, r^*, \rho(s_0), \gamma \rangle$ , where  $\mathcal{S}$  is the state space,  $\mathcal{A}$  is the action space,  $\mathcal{T}(s'|s, a)$  is the transition distribution,  $r^* : \mathcal{S} \times \mathcal{A} \rightarrow \mathbb{R}$  is the true reward function,  $\rho(s_0)$  is the initial state distribution, and  $\gamma \in (0, 1]$  is a discount factor. Note that the  $r^*$  is only determined by the environment and task. Furthermore, we denote  $\pi(a|s)$  as the policy of the agent. At each step, the agent observes the state of the environment and selects an action from the action space. Then the state-action pair will be rewarded by the reward function. Based on the MDP, we first define the objective of the RL.

**Definition 1 (RL).** *Given the MDP  $\mathcal{M}$ , the objective of the RL is to find the optimal policy  $\pi^*$  that maximizes the expected discounted reward:*

$$\pi^* = \operatorname{argmax}_{\pi \in \Pi} \mathbb{E}_{\tau \sim \pi} J(\pi|r^*), \quad (1)$$

where  $J(\pi|r^*) = \sum_{t=0}^{T-1} \gamma^t r_t^*(s_t, a_t)$ ,  $\Pi$  being the set of all stationary policies, and  $\tau = (s_0, a_0, \dots, a_{T-1}, s_T)$  being the trajectory generated by the policy.

On the contrary, the conventional IRL aims to learn a reward function that explains the observed behavior [4]. Given a set of trajectories  $\mathcal{D} = \{\tau_1, \dots, \tau_N\}$  which are assumed to be drawn from a demonstrator, then the IRL problem can be defined as:

**Definition 2 (IRL).** *Given the MDP  $\mathcal{M}$  and a set of trajectories  $\mathcal{D} = \{\tau_1, \dots, \tau_N\}$ , the objective of the IRL can be formulated as solving a maximum likelihood estimation (MLE) problem [11]:*

$$\max_{\theta} \mathbb{E}_{\tau \sim \mathcal{D}} [\log p_{\theta}(\tau)], \quad (2)$$

where  $p_{\theta}(\tau) \propto \rho(s_0) \prod_{t=0}^T \mathcal{T}(s_{t+1}|s_t, a_t) e^{\gamma^t r_{\theta}(s_t, a_t)}$ , and the  $r_{\theta}(s_t, a_t)$  is the parameterized reward function.

Such objective simply aims to imitate the policy of the expert, which can not learn a BD policy. In this paper, we aim to obtain the BD policy through the IRL. Denote by  $\hat{\pi}$  and  $\check{\pi}$  the generation policy and demonstrator policy respectively, we say that the the  $\hat{\pi}$  outperforms the  $\check{\pi}$  if:

$$J(\hat{\pi}|r^*) > J(\mathcal{D}|r^*), \quad (3)$$

where  $J(\mathcal{D}|r^*) = \frac{1}{|\mathcal{D}|} \sum_{\tau \in \mathcal{D}} J(\tau|r^*)$  is the estimation of the expected return of the  $\check{\pi}$ . Finally, we can define the BD-IRL as:

**Definition 3 (BD-IRL).** *Given the MDP  $\mathcal{M}$  and a set of trajectories  $\mathcal{D} = \{\tau_1, \dots, \tau_N\}$ , the objective of the BD-IRL is to find a policy  $\hat{\pi}$ :*

$$\hat{\pi} = \operatorname{argmax}_{\hat{\pi} \in \Pi} J(\hat{\pi}|r^*), \quad (4)$$

such that

$$J(\hat{\pi}|r^*) > J(\mathcal{D}|r^*). \quad (5)$$

It is intractable to straightforwardly obtain the optimal generation policy  $\hat{\pi}$ . The following section proposes a one-stage BD-IRL algorithm, which learns a hybrid reward function and realizes both the imitation and BD performance within a unified architecture.

## 4 Hybrid Adversarial Inverse Reinforcement Learning

In this section, we propose a hybrid adversarial inverse reinforcement learning (HAIRL) framework, which is a one-stage, model-free, GA fashion, and curiosity-driven IRL framework. The architecture of the HAIRL is illustrated in Fig. 1, which has two major components: the extrinsic reward block (ERB) and the intrinsic reward block (IRB). The ERB generates an ERS based on the demonstrations GA fashion, which leads the agent to approach the demonstrator policy rapidly. Meanwhile, the IRB generates an IRS using curiosity block, leading the agent to explore further to achieve BD performance. The two components are elaborated in detail in the following contents. Finally, the ERS and IRS collectively forms a hybrid reward for the policy updates.

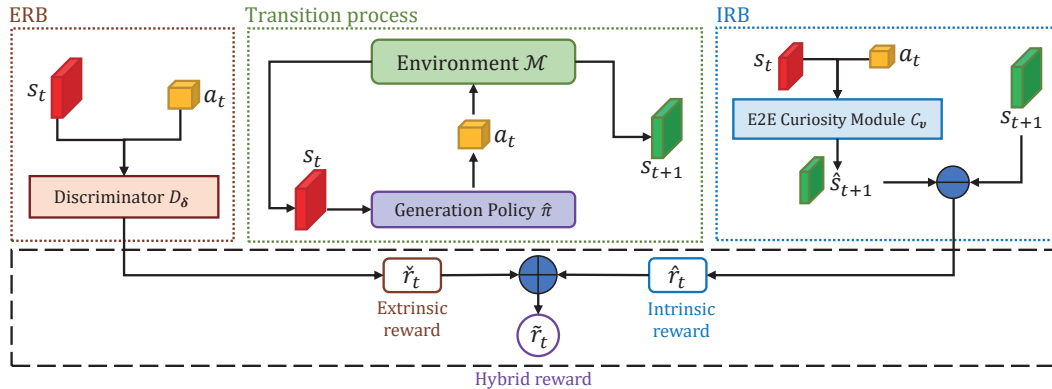


Figure 1: The architecture of the HAIRL, where  $\oplus$  denotes the add operation and  $\ominus$  denotes the Euclidean distance.

### 4.1 Extrinsic Reward Block

We build the ERB following the GA fashion proposed in AIRL [21]. For a standard GA structure, there is a generator for capturing the true data distribution, while a discriminator for estimating the probability that a sample belongs to the true data rather than the generated data [20]. However, the original GA fashion suffers from two critical challenges. On the one hand, the discriminator and generator are trained using binary cross-entropy as the loss function. It can not accurately reflect the distance between the true and generated data distribution and may lead to the gradient vanishing of the generator. On the other hand, the original loss function is proven to define an ambiguous objective for the generator, so it is likely to cause the model collapse [31].

To cope with the problems, we introduce the Wasserstein-1 distance (WD) to design the ERB, which induces the popular Wasserstein GAN in [32]. In sharp contrast to the original loss function, the WD can measure the distance between any two data distributions, providing stable gradients and overcoming the problems of model collapse and model generalization. We first define the WD:

**Definition 4 (WD).** Let  $\mathcal{X}$  be a compact set,  $P_r, P_g$  are two probability distributions which belong to the space of probability measures defined on  $\mathcal{X}$ , the WD between  $P_r$  and  $P_g$  is defined as [32]:

$$W(P_r, P_g) = \inf_{P_c \sim \Gamma(P_r, P_g)} \mathbb{E}_{(x, y) \sim P_c} [||x - y||], \quad (6)$$

where  $\Gamma(P_r, P_g)$  is the set of all joint distributions whose marginals are  $P_r, P_g$  respectively.

It is intractable to straightforwardly calculate the WD, but it can be transformed into an computable form based on Kantorovich-Rubinstein duality [33]:

$$\begin{aligned} W(P_r, P_g) &= \sup_{\|f\|_L \leq 1} \mathbb{E}_{x \sim P_r}[f(x)] - \mathbb{E}_{x \sim P_g}[f(x)] \\ &\approx \max_{\|f\|_L \leq 1} \mathbb{E}_{x \sim P_r}[f(x)] - \mathbb{E}_{x \sim P_g}[f(x)], \end{aligned} \quad (7)$$

where  $f : \mathcal{X} \rightarrow \mathbb{R}$  is 1-Lipschitz function. Therefore, we can construct a family of parameterized functions to approximate the supremum. In practice, such function can be represented as a deep neural network (DNN). In ERB, the generation policy  $\hat{\pi}$  serves as the generator, interacting with environment and producing trajectories. Given a trajectory  $\tau = (s_0, a_0, \dots, a_{T-1}, s_T)$ , we represent the discriminator  $D_\delta$  by as DNN with parameters  $\delta$ , and  $\delta$  is clipped into  $[-\zeta, \zeta]$ ,  $\zeta \in \mathbb{R}^+$  to satisfy the Lipschitz condition. Denote by  $\hat{\pi}(\tau) = \rho(s_0) \prod_{t=0}^{T-1} \mathcal{T}(s_{t+1}|s_t, a_t) \hat{\pi}(a_t|s_t)$  the trajectory distribution induced by the  $\hat{\pi}$ , the discriminator is trained to minimize the following loss function to approximate the  $W(\mathcal{D}, \hat{\pi}(\tau))$ :

$$L(\delta) = \sum_{i=0}^{T-1} \mathbb{E}_{\hat{\pi}(\tau)}[D_\delta(s_t, a_t)] - \sum_{i=0}^{T-1} \mathbb{E}_{\mathcal{D}}[D_\delta(s_t, a_t)]. \quad (8)$$

To decrease the WD between  $\mathcal{D}$  and  $\hat{\pi}(\tau)$ , we define an ERS  $\check{r}$  for the generation policy:

$$\check{r}_\delta(s_t, a_t) = \mathbb{E}_{\hat{\pi}(\tau)}[D_\delta(s_t, a_t)]. \quad (9)$$

More specifically, we prove that the demonstrator policy  $\check{\pi}$  can be learned by optimizing Eq. (1) using Eq. (9), which induces the following theorem:

**Theorem 1** (Consistency). *Given the MDP  $\mathcal{M}$  and a set of trajectories  $\mathcal{D} = \{\tau_1, \dots, \tau_N\}$ , the demonstrator policy can be learned via minimizing the loss function Eq. (8) while maximizing the discounted return with reward function Eq. (9).*

*Proof.* See the proof in Appendix A. □

The ERB learns from the sampled trajectories, which is inevitably influenced by the quantity and quality of the trajectories. Regardless of the BD objective, the ERB can be regarded as an independent IRL algorithm for imitating the demonstrator. However, most former IRL work barely discuss the sample complexity of the algorithm. Here we introduce the following theorem to roughly analyze the sample complexity of our ERB. The ERB actually minimizes the WD between  $\mathcal{D}$   $\hat{\pi}(\tau)$ , so we only need to analyze the sample complexity of minimizing the WD.

**Theorem 2** (Sample Complexity). *Given demonstration set  $\mathcal{D}$ , with probability at least  $1 - \kappa$ , the ERB recovers a policy  $\hat{\pi}$  such that:*

$$\max_{\|f\|_L \leq 1} \mathbb{E}_{s, a \sim \mathcal{D}}[f(s, a)] - \mathbb{E}_{s, a \sim \hat{\pi}(\tau)}[f(s, a)] \leq 4 \sqrt{\frac{2 \ln(|\Pi|) - \ln(\kappa)}{M}}, \quad (10)$$

where  $f$  is Lipschitz-1 function,  $M$  is the quantity of the state-action pairs in  $\mathcal{D}$ , and  $|\Pi|$  is the cardinality of the policy set.

*Proof.* See the proof in Appendix B □

The Theorem 2 indicates that the left hand side of the inequality has no dependency on the specific form of the  $f$ . It is only determined by the cardinality of the policy set and sample set. Given a policy set, the theorem also shows that more samples make the imitation more accurate.

## 4.2 Intrinsic Reward Block

Through the ERS, the generation policy can rapidly approach the demonstrator policy. Meanwhile, the agent is expected to explore the environment further to get BD performance. Making explorations depends on the curiosity of the agent, so we introduce the CM to provide an IRS for the agent. Fig. 2 illustrates the architecture of the ICM and ECM. Both of them generate the IRS based on the

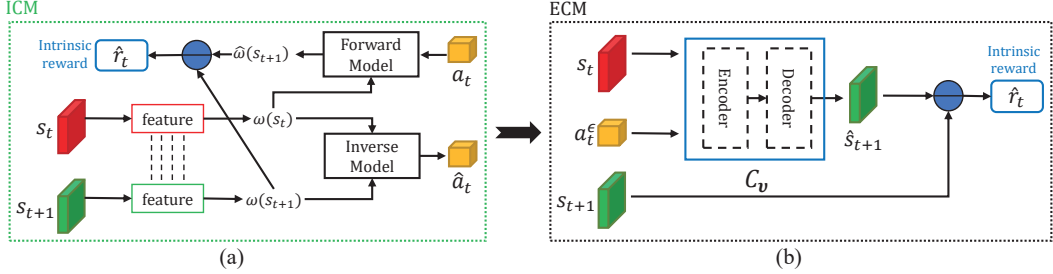


Figure 2: The architecture of the ICM and ECM,  $\omega(\cdot)$  denotes the encoding for the state space, and  $\ominus$  denotes the Euclidean distance.

uncertainty for the agent to predict the consequent actions. In ICM, the IRS is defined as the square of the Euclidean distance (ED) between the true next-state  $s_{t+1}$  and predicted next-state  $\hat{s}_{t+1}$ :

$$\hat{r}_t = \frac{1}{2} \|\omega(\hat{s}_{t+1}) - \omega(s_{t+1})\|_2^2. \quad (11)$$

The Eq. (11) indicates that if a predicted next-state produces more prediction error, the agent should pay more attention to the unfamiliar transition. By fully exploring these novel transitions, the agent can traverse more states to increase the probability of getting a higher performance. Such accident is the key insight for extrapolating BD performance.

To provide powerful and robust IRS, we develop a novel end-to-end curiosity module (ECM). There are two improvements in ECM in contrast to ICM. On the one hand, the ICM needs to encode the state space, which will be intractable and produces much variance in the high-dimension space (e.g. image space). The ECM drops the encoding procedure and realizes the end-to-end training to decrease the variance. On the other hand, the ICM uses two modules to reconstruct the transition process, which brings high computation complexity. The ECM only uses one DNN to accept states and actions and straightforwardly outputs the predicted next-state  $\hat{s}_{t+1}$ . Note that the encoder and decoder represent the two parts of the network, which are responsible for downsampling and upsampling, respectively. In particular, we use an  $\epsilon$ -greedy actions  $a_t^\epsilon$  to let the ECM see more state-action pairs, which aims to improve the generalization of the ECM:

$$P(a_t^\epsilon) = \begin{cases} \frac{\epsilon}{|\mathcal{A}|}, a_t^\epsilon \sim \mathcal{A} \\ 1 - \epsilon + \frac{\epsilon}{|\mathcal{A}|}, a_t^\epsilon = a_t \end{cases}, \quad (12)$$

where  $P(\cdot)$  denotes the probability and  $|\mathcal{A}|$  is the cardinality of the action space. In training, this trick will randomly select an action from the  $\mathcal{A}$  to replace the original action with a probability of  $\epsilon$ . Given a trajectory  $\tau = (s_0, a_0, \dots, a_{T-1}, s_T)$ , we represent the ECM  $C_v$  by a DNN with parameters  $v$ , the ECM is trained to minimize the following loss function:

$$L(v) = \sum_{t=0}^{T-1} \frac{1}{2} \|C_v(s_t, a_t) - s_{t+1}\|_2^2. \quad (13)$$

Finally, the IRS takes the same form in Eq. (11) without the encoding operation:

$$\hat{r}_v(s_t, a_t, s_{t+1}) = \frac{1}{2} \|C_v(s_t, a_t) - s_{t+1}\|_2^2. \quad (14)$$

### 4.3 Hybrid Reward for BD Learning

So far the ERB and the IRB are obtained respectively, the two elements collectively build the hybrid reward as follows:

$$\tilde{r}(s_t, a_t, s_{t+1}) = \alpha \cdot \check{r}_\theta + \beta \cdot \hat{r}_v, \quad (15)$$

where the  $\alpha, \beta \in [0, 1]$  is the weighting scalar that weights the extrinsic reward against the intrinsic reward. Note that the range of the IRS and ERS might be different due to their procedure, so standardization operation should be considered in practice. After the hybrid reward is obtained, the generation policy  $\hat{\pi}$  can be updated using any policy optimization method. Finally, the workflow of the HAIRL is summarized in Algo. 1.

---

**Algorithm 1** Hybrid Adversarial Inverse Reinforcement Learning

---

- 1: Obtain expert demonstrations  $\mathcal{D}$ ;
- 2: Initialize the generation policy network  $\hat{\pi}$ , discriminator  $D_\delta$  and ECM  $C_v$ ;
- 3: Initialize the weighting scalar  $\alpha, \beta$  and probability scalar  $\epsilon$ ;
- 4: **for** epoch  $e = 1, \dots, E$  **do**
- 5:   Execute policy  $\hat{\pi}$  and collect the trajectory  $\tau_e = (s_0, a_0, \dots, a_{T-1}, s_T)$ ;
- 6:   Train the discriminator by minimizing the following loss function:

$$L(\delta) = \sum_{i=0}^{T-1} \mathbb{E}_{\hat{\pi}(\tau)}[D_\delta(s_t, a_t)] - \sum_{i=0}^{T-1} \mathbb{E}_{\mathcal{D}}[D_\delta(s_t, a_t)];$$

- 7:   Train the ECM by minimizing the following loss:

$$L(v) = \sum_{t=0}^{T-1} \frac{1}{2} \|C_v(s_t, a_t) - s_{t+1}\|_2^2;$$

- 8:   Calculate the hybrid reward for each state-action pair in  $\tau_e$ :

$$\tilde{r}(s, a, s') = \alpha \cdot \mathbb{E}_{\hat{\pi}(\tau)}[D_\delta(s, a)] + \beta \cdot \frac{1}{2} \|C_v(s, a) - s'\|_2^2;$$

- 9:   Update  $\hat{\pi}$  with respect to the hybrid reward using any policy optimization method.

- 10: **end for**

---

## 5 Experimental Evaluation

In this section, we will evaluate the HAIRL on multiple games in in OpenAI Gym library [34]. In particular, we introduce the Atari games of the Gym whose state space are composed of images, which aims to testify the robustness of HAIRL to high-dimensional state space. Table 1 illustrates the details of the selected games.

Table 1: The details of the Atari games.

Game	Observation shape	Action space size
Breakout	(84,84,4)	4
Space Invaders	(84,84,4)	6
Q*Bert	(84,84,4)	6
Beam Rider	(84,84,4)	9
Kung Fu Master	(84,84,4)	14
Seaquest	(84,84,4)	18

For benchmarking, we select several representative algorithms to serve as the benchmarks, which are GIRIL, TREX, Curiosity-driven imitation learning (CDIL) in [7] and adversarial inverse reinforcement learning (AIRL) in [21]. The former two frameworks are two-stage BD-IRL algorithms, while the latter two belong to imitation learning algorithms. With GIRIL and TREX, we can compare the efficiency between the one-stage algorithms and the two-stage algorithms. With AIRL and CDIL, we can testify that whether the HAIRL can imitate and outperform the demonstrator. To make a fair comparison, all the methods are required to use the same architecture for the policy network.

### 5.1 Expert Demonstrations

To get expert demonstrations, we use proximal policy optimization (PPO) to train expert agents with the true reward [35]. The agent is set to interact with the environment for 10 million steps. Specifically, we use the Pytorch implementation of the PPO created by [36], and other hyper-parameters are set as default. After the expert agents are obtained, it is used to generate expert demonstrations with randomly initialized environments.

## 5.2 Experimental Setup

Since the state space of the Atari games is composed of images, so the convolutional neural network (CNN) is used to build the HAIRL. The detailed network architectures of the all the components in HAIRL can be found in Appendix C.

We train the HAIRL for 10 thousand epochs. In each epoch, the agent needs to interact with 8 parallel environments for 128 steps, producing 1024 pieces of transitions. Firstly, the transitions are leveraged to update the discriminator  $D_\delta$ . More specifically, the batch size is set as 256, and the RMSprop optimizer is used to apply the gradient descent, which uses a linearly decaying learning rate. In particular, the gradients and weights are clipped into  $[-5, 5]$  and  $[-0.1, 0.1]$ . It satisfies the requirement for approximating the WD and stabilize the training process. Secondly, we use the generated transitions to train the ECM. The ECM accepts an image with shape  $(84, 84, 4)$ , and it is downsampled to produce a feature vector. Immediately, the feature vector is concatenated with the one-hot action, which is processed by the latter part of  $C_v$  to regenerate a  $(84, 84, 4)$  image. The batch size is set as 256 and the learning rate also decays linearly, but we use Adam optimizer in [37] to apply gradients descent.

After the ERB and IRB are updated, they are used to calculate hybrid reward for the transitions, where  $\alpha = 0.01$  and  $\beta = 0.99$ . The PPO immediately accepts the transitions with hybrid rewards to update the generation policy  $\hat{\pi}$ . As for the training of the benchmark algorithms, we follow the default setups in its literature.

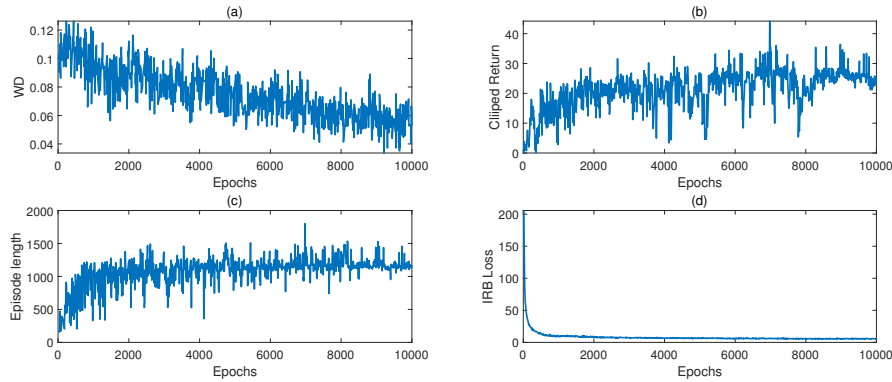


Figure 3: Training diagram of the Space Invaders game.

## 5.3 Results

Take the Space Invaders game for instance, Fig. 3 illustrates the variation of four metrics in training. As shown in the figure, the WD between demonstrator and generation policy decreases stably, which means that the generation policy keeps approaching the demonstrator. Meanwhile, the IRB takes few epochs to realize the convergence, which demonstrates the high efficiency of the proposed ECM. Finally, the average return and episode length of the agent also improve stably, which indicates that the agent can survive longer time and achieve higher performance in the game.

Next, we compare the performance of the HAIRL against the benchmark algorithms. We take the normalized average one-life return as the key performance indicator (KPI), in which the reward values are normalized into  $[0, 1]$  and the agent interacts with the environments initialized by 5 random seeds. Table 2 illustrates the performance comparison of the HAIRL and benchmarks, in which the BD performance is in bold. For instance, the "33.8/616" in the third row and first column means the algorithm takes 616 average steps to achieve a 33.8 average return.

As shown in Table 2, the HAIRL successfully outperforms the expert agent in 5 games, producing 13.72 average gain performance. In contrast, the TREX and GIRL outperform the expert agent in 4 and 2 games, respectively. For imitation algorithms CDIL and AIRL, the CDIL achieves BD performance in 1 game, while the AIRL fails in all games. In the Q\*Bert game, all the algorithms fail to outperform the expert, but the HAIRL still achieves the highest score. With simpler architecture

Table 2: Average return comparison in Atari games.

Game	Expert	One-stage		Two-stage		
	Average	HARIL	AIRL	GIRIL	CDIL	TREX
Space Invaders	33.8/616	<b>36.4/1443</b>	17.0/330	19.6/1043	25.2/1123	32.2/1441
Breakout	51.8/1134	<b>60.2/1485</b>	0.8/49	37.6/1021	<b>56.4/1211</b>	<b>53.0/1207</b>
Beam Rider	18.2/2057	<b>50.0/5604</b>	6.8/987	<b>44.7/4095</b>	2.8/1616	<b>28.8/8934</b>
Q*Bert	121.8/733	77.6/12116	3.7/141	30.7/56550	22.6/10905	43.0/7892
Kung Fu Master	28.2/671	<b>51.8/1541</b>	0.5/241	<b>42.4/1391</b>	12.6/569	<b>40.6/1226</b>
Seaquest	12.0/559	<b>14.2/808</b>	1.0/153	9.0/510	9.8/559	<b>13.1/757</b>

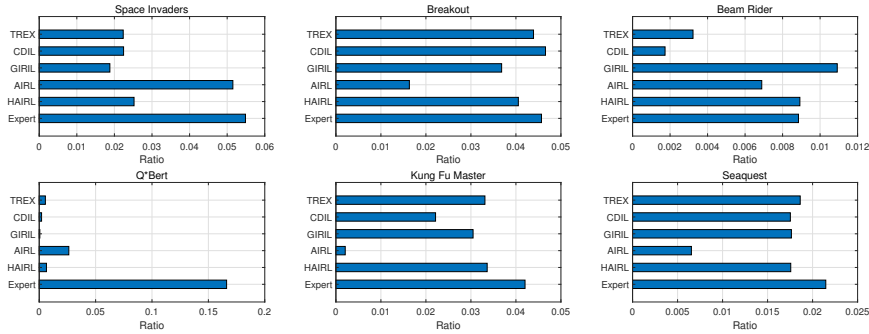


Figure 4: The ratio between average return and average steps.

and fewer computations, the HAIRL obtains excellent efficiency and realizes higher performance. Furthermore, we calculate the ratio between the average return and average steps, which is shown in Fig. 4. It is evident that the experts realize the same performance with fewer steps in most games, especially in the Q\*Bert game. This reflects the procrastination of the curiosity-driven RL agents, which is first reported in the [38]. Under the supervision of the curiosity module, the agent will strive to explore all possible states even though some states are useless. Therefore, these algorithms usually achieve the same performance at the cost of more steps when compared with the expert. In HAIRL, the ERS can lead the agent to imitate the expert policy and correct the influence of the IRS. For instance, if a transition produces a high IRS and a high ERB instantaneously, the ERB can intensify the motivation of the agent to explore the high-potential states. On the opposite, if the agent wastes much time on the same states, the ERS will prevent the agent from staying by reducing the rewards. In a word, the HAIRL is more adaptive and robust when handling complex conditions.

## 6 Conclusion

In this paper, we have investigated the problem of the BD-IRL. To realize efficient and robust BD-IRL, we propose a one-stage, generative-adversarial fashion and curiosity-driven framework entitled hybrid adversarial inverse reinforcement learning, which integrates the reward function learning and policy optimization into one procedure. In HAIRL, we skillfully design two modules that collectively generate hybrid rewards for the agent to imitate the demonstrator and extrapolate BD performance. In particular, we design a novel curiosity module that provides powerful exploration motivation with simple architecture and high efficiency. Finally, we evaluate the HAIRL on multiple Atari games, and the simulation results show that the HAIRL outperforms the similar SOTA algorithms.

## A Proof of Theorem 1

The ERB simply aims to imitate the demonstrator policy, which is consistent with the objective defined in Eq. (2). Let:

$$\max_{\theta} I(\theta) = \max_{\theta} \mathbb{E}_{\tau \sim \mathcal{D}} [\log p_{\theta}(\tau)],$$

where  $p_{\theta}(\tau) \propto \rho(s_0) \prod_{t=0}^T \mathcal{T}(s_{t+1}|s_t, a_t) e^{\gamma^t r_{\theta}(s_t, a_t)}$ . The demonstrations satisfy the Boltzmann distribution [11][39]:

$$p_{\theta}(\tau) = \frac{1}{Z_{\theta}} \exp\left\{\sum_{s_t, a_t \in \tau} r_{\theta}(s_t, a_t)\right\} = \frac{1}{Z_{\theta}} \tilde{p}_{\theta}(\tau),$$

where  $\tilde{p}_{\theta}$  is the unnormalized probability distribution and  $Z_{\theta} = \int_{\tau} \tilde{p}_{\theta}(\tau) d\tau$  is the partition function. Taking the gradient of the  $I(\theta)$  with respect to  $\theta$ :

$$\nabla_{\theta} I(\theta) = \mathbb{E}_{\mathcal{D}}[\nabla_{\theta} \log p_{\theta}(\tau)] = \mathbb{E}_{\mathcal{D}}\left[\sum_{t=0}^T \nabla_{\theta} r_{\theta}(s_t, a_t)\right] - \nabla_{\theta} \log Z_{\theta}.$$

We further analyze the gradient of the  $Z_{\theta}$ , [40] proves that:

$$\nabla_{\theta} \log Z_{\theta} = \mathbb{E}_{p_{\theta}} \nabla_{\theta} \log \tilde{p}_{\theta}.$$

Finally, the gradient can be written as:

$$\begin{aligned} \nabla_{\theta} I(\theta) &= \mathbb{E}_{\mathcal{D}}\left[\sum_{t=0}^T \nabla_{\theta} r_{\theta}(s_t, a_t)\right] - \mathbb{E}_{p_{\theta}}\left[\sum_{t=0}^T \nabla_{\theta} r_{\theta}(s_t, a_t)\right] \\ &= \sum_{t=0}^T \mathbb{E}_{\mathcal{D}}\left[\nabla_{\theta} r_{\theta}(s_t, a_t)\right] - \mathbb{E}_{p_{\theta,t}}\left[\nabla_{\theta} r_{\theta}(s_t, a_t)\right], \end{aligned} \quad (16)$$

where  $p_{\theta,t}(s_t, a_t) = \int_{s_{t'} \neq t, a_{t'} \neq t} p_{\theta}(\tau)$  be the state-action marginal at time  $t$ . It is intractable to straightforwardly get samples from  $p_{\theta,t}$ , so we apply the importance sampling method to estimate its expectation [41]. Finally, the gradient is rewritten as:

$$\nabla_{\theta} I(\theta) = \sum_{t=0}^T \mathbb{E}_{\mathcal{D}}\left[\nabla_{\theta} r_{\theta}(s_t, a_t)\right] - \mathbb{E}_{\mu_t}\left[\frac{p_{\theta,t}(s_t, a_t)}{\mu_t(s_t, a_t)} \nabla_{\theta} r_{\theta}(s_t, a_t)\right], \quad (17)$$

where  $\mu(\tau) = \sigma(s_0) \prod_{t=0}^{T-1} \mathcal{T}(s_{t+1}|s_t, a_t) \mu(a_t|s_t)$  is the sampling distribution. Meanwhile, we need to reduce the variance of importance sampling. The optimal sampling distribution satisfies:

$$\mu_{\tau} \propto \exp\left\{\sum_{s_t, a_t \in \tau} r_{\theta}(s_t, a_t)\right\}.$$

So the sampler  $\mu(s_t, a_t)$  is asked to maximize the following objective to approach the demonstrator policy:

$$\mathbb{E}_{\tau \sim \mu(\tau)} \sum_{t=0}^T r_{\theta}(s_t, a_t). \quad (18)$$

Finally, the demonstrator policy can be learned by alternately optimizing the Eq. (17) and Eq. (18). Next, we observe the loss function Eq. (8), the gradient of its opposite form is:

$$\nabla_{\delta} L(\delta) = \sum_{t=0}^T \mathbb{E}_{\mathcal{D}}\left[\nabla_{\delta} D_{\delta}(s_t, a_t)\right] - \mathbb{E}_{\hat{p}_t}\left[\nabla_{\delta} D_{\delta}(s_t, a_t)\right], \quad (19)$$

where  $\hat{p}_t(s_t, a_t) = \int_{s_{t'} \neq t, a_{t'} \neq t} \hat{\pi}(\tau)$  is the state-action marginal induced by  $\hat{\pi}$ . The Eq. (19) is consistent with the Eq. (17). Since the  $\hat{\pi}$  also needs to maximize the inferred reward function to reduce the WD with the demonstrator policy, thus the two learning process is consistent which concludes the proof.

## B Proof of Theorem 2

Define a set  $\mathcal{F}$  of Lipschitz-1 functions, for two policy  $\pi, \pi' \in \Pi, \pi \neq \pi'$ , such that:

$$f := \underset{\|f\|_L \leq 1}{\text{argmax}} \left[ \mathbb{E}_{s, a \sim \pi}[f(s, a)] - \mathbb{E}_{s, a \sim \pi'}[f(s, a)] \right], \quad (20)$$

where  $f \in \mathcal{F}$ ,  $|\mathcal{F}| \leq |\Pi|^2$ . Given trajectory set  $\mathcal{D}$  that contains  $M$  state-action pairs, minimizing the WD between  $\hat{\pi}$  and  $\mathcal{D}$  is equivalent to the following optimization problem:

$$\hat{\pi} = \operatorname{argmin}_{\pi \in \Pi} \left[ \max_{f \in \mathcal{F}} \left[ \frac{1}{M} \sum_{i=1}^M f(s_i, a_i) - \mathbb{E}_{s, a \sim \pi} f(s, a) \right] \right], \quad (21)$$

where  $(s_i, a_i) \in \mathcal{D}$  and  $\frac{1}{M} \sum_{i=1}^M f(s_i, a_i)$  is the estimation of the  $\mathbb{E}_{s, a \sim \mathcal{D}} f(s, a)$ . The Hoeffding's inequality in [42], for all  $f \in \mathcal{F}$ , it holds:

$$\left| \frac{1}{M} \sum_{i=1}^M f(s_i, a_i) - \mathbb{E}_{s, a \sim \mathcal{D}} f(s, a) \right| \leq 2 \sqrt{\frac{\ln(|\mathcal{F}|/\kappa)}{M}} = \epsilon.$$

Let

$$\begin{aligned} \hat{f} &:= \operatorname{argmax}_{f \in \mathcal{F}} \left[ \mathbb{E}_{s, a \sim \mathcal{D}} [f(s, a)] - \mathbb{E}_{s, a \sim \hat{\pi}} [f(s, a)] \right], \\ \tilde{f} &:= \operatorname{argmax}_{f \in \mathcal{F}} \left[ \frac{1}{M} \sum_{i=1}^M f(s_i, a_i) - \mathbb{E}_{s, a \sim \hat{\pi}} f(s, a) \right]. \end{aligned}$$

Then

$$\begin{aligned} \max_{\|f\|_L \leq 1} \mathbb{E}_{s, a \sim \mathcal{D}} [f(s, a)] - \mathbb{E}_{s, a \sim \hat{\pi}} [f(s, a)] \\ &= \mathbb{E}_{s, a \sim \mathcal{D}} [\hat{f}(s, a)] - \mathbb{E}_{s, a \sim \hat{\pi}} [\hat{f}(s, a)] \\ &\leq \epsilon + \frac{1}{M} \sum_{i=1}^M \tilde{f}(s_i, a_i) - \mathbb{E}_{s, a \sim \hat{\pi}} [\tilde{f}(s, a)] \\ &\leq \epsilon + \frac{1}{M} \sum_{i=1}^M \tilde{f}(s_i, a_i) - \mathbb{E}_{s, a \sim \mathcal{D}} [\tilde{f}(s, a)] \\ &\leq 2\epsilon \leq 4 \sqrt{\frac{2 \ln(|\Pi|) - \ln(\kappa)}{M}}, \end{aligned}$$

where the second inequality follows the fact that  $\hat{\pi}$  is the minimizer of the Eq. (21). This concludes the proof.

## C Experimental Setup

Table 3 illustrates the detailed architectures deployed in our experiments, where each convolutional layer is followed by a batch normalization (BN) layer, and the Flatten layer is to convert a tensor into a vector. Finally, the ConvTranspose is a special convolutional operation for upsampling.

Table 3: The CNN-based architectures of the modules.

Module	$\hat{\pi}$	$D_\delta$	$C_v$
Input	States	States and one-hot actions	States and one-hot actions
Arch.	8×8 Conv 32, ReLU	8×8 Conv 32, Tanh	8×8 Conv 32, ReLU
	4×4 Conv 64, ReLU	4×4 Conv 64, Tanh	4×4 Conv 64, ReLU
	3×3 Conv 32, ReLU	3×3 Conv 32, Tanh	3×3 Conv 32, ReLU
	Flatten	Flatten	Flatten
	Dense 512, ReLU	Dense 128+  $\mathcal{A}$  , Tanh	Dense 32*11*11
	Dense   $\mathcal{A}$	Dense 1	Reshape to (32,11,11)
Categorical Distribution			ConvTranspose 32, ReLU
			ConvTranspose 32, ReLU
			ConvTranspose 32
Output	Actions	Scores	Predicted next-states

## References

- [1] David Silver, Thomas Hubert, Julian Schrittwieser, Ioannis Antonoglou, Matthew Lai, Arthur Guez, Marc Lanctot, Laurent Sifre, Dharshan Kumaran, Thore Graepel, et al. A general reinforcement learning algorithm that masters chess, shogi, and go through self-play. *Science*, 362(6419):1140–1144, 2018.
- [2] Oriol Vinyals, Igor Babuschkin, Wojciech M Czarnecki, Michaël Mathieu, Andrew Dudzik, Junyoung Chung, David H Choi, Richard Powell, Timo Ewalds, Petko Georgiev, et al. Grandmaster level in starcraft ii using multi-agent reinforcement learning. *Nature*, 575(7782):350–354, 2019.
- [3] Andrew Y Ng, Daishi Harada, and Stuart Russell. Policy invariance under reward transformations: Theory and application to reward shaping. In *Icml*, volume 99, pages 278–287, 1999.
- [4] Andrew Y Ng, Stuart J Russell, et al. Algorithms for inverse reinforcement learning. In *Icml*, volume 1, page 2, 2000.
- [5] Richard S Sutton and Andrew G Barto. *Reinforcement learning: An introduction*. MIT press, 2018.
- [6] Daniel S Brown, Wonjoon Goo, Prabhat Nagarajan, and Scott Niekum. Extrapolating beyond suboptimal demonstrations via inverse reinforcement learning from observations. *arXiv preprint arXiv:1904.06387*, 2019.
- [7] Xingrui Yu, Yueming Lyu, and Ivor Tsang. Intrinsic reward driven imitation learning via generative model. In *International Conference on Machine Learning*, pages 10925–10935. PMLR, 2020.
- [8] Sili Huang, Bo Yang, Hechang Chen, Haiyin Piao, Zhixiao Sun, and Yi Chang. Ma-trex: Multi-agent trajectory-ranked reward extrapolation via inverse reinforcement learning. In *International Conference on Knowledge Science, Engineering and Management*, pages 3–14. Springer, 2020.
- [9] Daniel S Brown, Wonjoon Goo, and Scott Niekum. Better-than-demonstrator imitation learning via automatically-ranked demonstrations. In *Conference on Robot Learning*, pages 330–359. PMLR, 2020.
- [10] Diederik P Kingma and Max Welling. Auto-encoding variational bayes. *arXiv preprint arXiv:1312.6114*, 2013.
- [11] Brian D Ziebart, Andrew L Maas, J Andrew Bagnell, and Anind K Dey. Maximum entropy inverse reinforcement learning. In *Aaai*, volume 8, pages 1433–1438. Chicago, IL, USA, 2008.
- [12] Brian D Ziebart. Modeling purposeful adaptive behavior with the principle of maximum causal entropy. 2010.
- [13] Deepak Ramachandran and Eyal Amir. Bayesian inverse reinforcement learning. In *IJCAI*, volume 7, pages 2586–2591, 2007.
- [14] Dylan Hadfield-Menell, Anca Dragan, Pieter Abbeel, and Stuart Russell. Cooperative inverse reinforcement learning. *arXiv preprint arXiv:1606.03137*, 2016.
- [15] Sergey Levine, Zoran Popovic, and Vladlen Koltun. Nonlinear inverse reinforcement learning with gaussian processes. *Advances in neural information processing systems*, 24:19–27, 2011.
- [16] Markus Wulfmeier, Peter Ondruska, and Ingmar Posner. Deep inverse reinforcement learning. *arXiv preprint arXiv:1507.04888*, 2015.
- [17] Kareem Amin, Nan Jiang, and Satinder Singh. Repeated inverse reinforcement learning. *arXiv preprint arXiv:1705.05427*, 2017.
- [18] Sriraam Natarajan, Gautam Kunapuli, Kshitij Judah, Prasad Tadepalli, Kristian Kersting, and Jude Shavlik. Multi-agent inverse reinforcement learning. In *2010 Ninth International Conference on Machine Learning and Applications*, pages 395–400. IEEE, 2010.
- [19] Chelsea Finn, Paul Christiano, Pieter Abbeel, and Sergey Levine. A connection between generative adversarial networks, inverse reinforcement learning, and energy-based models. *arXiv preprint arXiv:1611.03852*, 2016.
- [20] Ian Goodfellow, Jean Pouget-Abadie, Mehdi Mirza, Bing Xu, David Warde-Farley, Sherjil Ozair, Aaron Courville, and Yoshua Bengio. Generative adversarial nets. *Advances in neural information processing systems*, 27:2672–2680, 2014.

- [21] Justin Fu, Katie Luo, and Sergey Levine. Learning robust rewards with adversarial inverse reinforcement learning. *arXiv preprint arXiv:1710.11248*, 2017.
- [22] Pierre-Yves Oudeyer and Frederic Kaplan. What is intrinsic motivation? a typology of computational approaches. *Frontiers in neurorobotics*, 1:6, 2009.
- [23] Marc Bellemare, Sriram Srinivasan, Georg Ostrovski, Tom Schaul, David Saxton, and Remi Munos. Unifying count-based exploration and intrinsic motivation. *Advances in neural information processing systems*, 29:1471–1479, 2016.
- [24] Manuel Lopes, Tobias Lang, Marc Toussaint, and Pierre-Yves Oudeyer. Exploration in model-based reinforcement learning by empirically estimating learning progress. In *Advances in neural information processing systems*, pages 206–214, 2012.
- [25] Rein Houthooft, Xi Chen, Yan Duan, John Schulman, Filip De Turck, and Pieter Abbeel. Vime: Variational information maximizing exploration. *Advances in neural information processing systems*, 29:1109–1117, 2016.
- [26] Yi Sun, Faustino Gomez, and Jürgen Schmidhuber. Planning to be surprised: Optimal bayesian exploration in dynamic environments. In *International Conference on Artificial General Intelligence*, pages 41–51. Springer, 2011.
- [27] Satinder Singh, Andrew G Barto, and Nuttapong Chentanez. Intrinsically motivated reinforcement learning. Technical report, MASSACHUSETTS UNIV AMHERST DEPT OF COMPUTER SCIENCE, 2005.
- [28] Bradly C Stadie, Sergey Levine, and Pieter Abbeel. Incentivizing exploration in reinforcement learning with deep predictive models. *arXiv preprint arXiv:1507.00814*, 2015.
- [29] Deepak Pathak, Pulkit Agrawal, Alexei A Efros, and Trevor Darrell. Curiosity-driven exploration by self-supervised prediction. In *Proceedings of the IEEE Conference on Computer Vision and Pattern Recognition Workshops*, pages 16–17, 2017.
- [30] Yuri Burda, Harri Edwards, Deepak Pathak, Amos Storkey, Trevor Darrell, and Alexei A Efros. Large-scale study of curiosity-driven learning. *arXiv preprint arXiv:1808.04355*, 2018.
- [31] Martin Arjovsky and Léon Bottou. Towards principled methods for training generative adversarial networks. *arXiv preprint arXiv:1701.04862*, 2017.
- [32] Martin Arjovsky, Soumith Chintala, and Léon Bottou. Wasserstein gan. *arXiv preprint arXiv:1701.07875*, 2017.
- [33] Cédric Villani. *Optimal transport: old and new*, volume 338. Springer Science & Business Media, 2008.
- [34] Greg Brockman, Vicki Cheung, Ludwig Pettersson, Jonas Schneider, John Schulman, Jie Tang, and Wojciech Zaremba. Openai gym. *arXiv preprint arXiv:1606.01540*, 2016.
- [35] John Schulman, Filip Wolski, Prafulla Dhariwal, Alec Radford, and Oleg Klimov. Proximal policy optimization algorithms. *arXiv preprint arXiv:1707.06347*, 2017.
- [36] Kostrikov. Pytorch implementation of the reinforcement learning algorithms. URL <https://github.com/ikostrikov/pytorch-a2c-ppo-acktr-gail>, 2018.
- [37] Diederik P Kingma and Jimmy Ba. Adam: A method for stochastic optimization. *arXiv preprint arXiv:1412.6980*, 2014.
- [38] Nikolay Savinov, Anton Raichuk, Raphaël Marinier, Damien Vincent, Marc Pollefeys, Timothy Lillicrap, and Sylvain Gelly. Episodic curiosity through reachability. *arXiv preprint arXiv:1810.02274*, 2018.
- [39] Yann LeCun, Sumit Chopra, Raia Hadsell, M Ranzato, and F Huang. A tutorial on energy-based learning. *Predicting structured data*, 1(0), 2006.
- [40] Yann LeCun, Yoshua Bengio, and Geoffrey Hinton. Deep learning. *nature*, 521(7553):436–444, 2015.
- [41] Alexander Shapiro. Monte carlo sampling methods. *Handbooks in operations research and management science*, 10:353–425, 2003.
- [42] Wassily Hoeffding. Probability inequalities for sums of bounded random variables. In *The Collected Works of Wassily Hoeffding*, pages 409–426. Springer, 1994.